EFFECTS OF EXPANSION IN THE WAKE ALIGNMENT OF HORIZONTAL AXIS TURBINES WITH A LIFTING LINE MODEL

Marcin Dolata

dol.marcin@gmail.com

Instituto Superior Técnico, Universidade de Lisboa, Portugal

January 2021

ABSTRACT

This work continues the development of the lifting line code, by taking first steps towards the application of the wake expansion effect in the wind turbine design procedure. The approach to the wake expansion, the relevant theory, and the necessary assumptions are presented along the way. The main goal of the conducted analysis is to explore effects of the newly introduced wake expansion with the use of the wake alignment procedure. The results are compared to the ones obtained without the application of the wake expansion and discussed in the light of the results and conclusions of previous contributors to the lifting line code. Convergence studies were performed, and converged solutions could be successfully obtained. However, when the wake alignment procedure is applied, the model is still sensitive to numerical disturbances and the input parameters should be chosen carefully. Interestingly, the introduction of the wake expansion in some cases improves the results' stability both in the overall behavior of the wake geometry and in the local variables distributions. This further translate into more reliable values of the power coefficient predicted by the wind turbine load design optimization with the lifting line model. From the conclusions, the reasons behind the encountered problems are discussed and the possible ways for future work on the lifting line code development are presented.

KEYWORDS: Wind Turbines; Lifting line theory; Wake Alignment; Wake Expansion; Optimization.

INTRODUCTION

The English engineer, Frederick W. Lanchester [1] and German mathematician, M. Wilhelm Kutta were the first to came up with a concept that there must be a connection between lift force and circulation. However, the one that derived a quantitative relation between lift and circulation was Russian scientist, Nikolai Y. Joukowski. He suggested the formula known as the "Kutta-Joukowski theorem":

$$\vec{L} = -\rho \vec{V}_\infty \times \vec{\Gamma}, \qquad (1)$$

where $\vec{L}$ is the lift force by unit span, ρ is the volumetric mass density of the fluid, $\vec{V}_\infty$ is the velocity of the undisturbed flow and $\vec{\Gamma}$ is the velocity circulation.

These bases of the lifting theory gave rise to many important and groundbreaking innovations in the fields of lifting surfaces such as propellers, wings turbines.

Throughout the years, there have been many contributions to the development of the lifting line theory. Moreover, the advancements in the computational science opened the door for application of numerical approach to the theory.

The introduction of the discretization made it possible to apply the wake alignment schemes. That allowed the modelling of the wakes with variable geometry by aligning it with the local velocities at multiple axial stations. As the numerical models are very sensitive to the disturbances, the correct modelling of the wake geometry has the enormous influence on the quality of the results.

The research group from IST in Lisbon, led by Falcao de Campos and Baltazar, has developed a lifting line code for the design and analysis of the horizontal axis wind turbines and propellers. Over the years of research, the code had many contributors. Machado [2] - [3] in 2010 used the effect of the hub in a design routine for marine turbines. In 2014 Caldeira [4] stimulated the effects of drag by implementing a source model. Melo [5] - [6] in 2016 included a wake alignment scheme. In 2018 Sousa [7] made the optimization procedure adjusting the analysis code by Melo and implementing the Lagrange multiplier method.

The next step towards the development of the lifting line code is complementing the wake alignment procedure with the effect of the wake expansion what theoretically should result in modeling more realistic wake geometries.

THEORY

System of vortices

Consider the rotor of a horizontal wind turbine rotating with constant angular velocity $\vec{\omega}$ in a uniform inflow field with velocity $\vec{U}$ aligned with the axis of rotation. The rotor has radius R and Z blades symmetrically distributed around the hub of radius r_h. We define a Cartesian coordinate system (x, y, z) and a cylindrical reference frame rotating with the rotor (x, r, θ) in which a relative velocity field is $\vec{U}_\infty = \vec{U} - \vec{\omega} \times \vec{r}$ as depicted in Fig. 1.

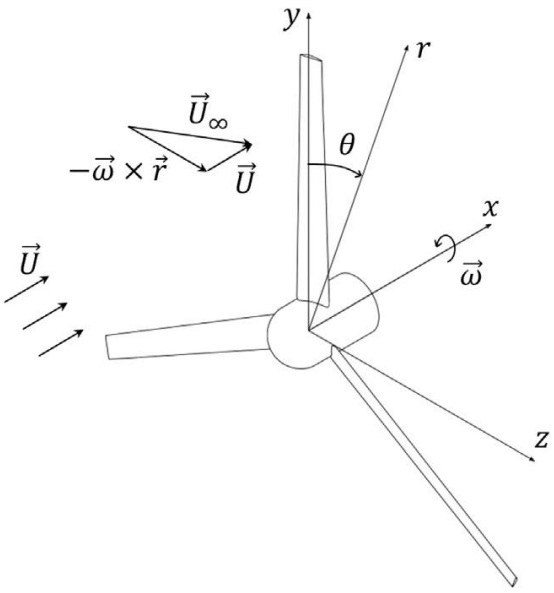

Fig. 1: Considered coordinate systems and uniform inflow velocity fields (from [5])

In the lifting line theory, the lifting body is modelled as a bound vortex called a lifting line. As already stated, lift force is proportional to circulation which in the potential flow can be represented by a vortex extending from the root to the tip, with coordinates:

$$r_h < r < R,\ \theta_k = \frac{2\pi(k-1)}{Z}, k = 1, \dots, Z. \tag{2}$$

This vortex is characterized by the spanwise variation of the circulation given by:

$$\vec{\Gamma}(r) = -\Gamma\,(r)\vec{e}_r, \tag{3}$$

where $\vec{e}_r$ is a radial unit vector. As circulation goes to zero at the blade tip and according to Helmholtz [8] theorem vortex cannot begin or terminate in a fluid, the variation of the circulation causes shedding of a sheet of trailing vortices from the lifting line downstream to the flow shown in Fig. 2. The intensity of this semi-infinite vortex sheet is proportional to this variation of circulation and expressed by:

$$\vec{\gamma} = \frac{d\Gamma\,(r)}{dr}\vec{e}_s, \tag{4}$$

where $\vec{e}_s$ is a unit vector tangent to the vortex sheet and aligned with the vortex filaments.

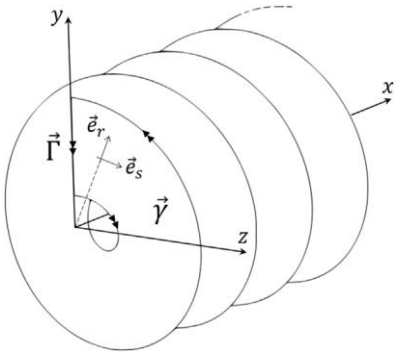

Fig. 2: System of vortices – single lifting line (from [5])

In the force-free wake the vortex filaments must be aligned with the local velocity field, so that:

$$\vec{\gamma} \times \vec{V} = 0. \tag{5}$$

Without considering the influence of the vortices, the velocity field in the rotating reference frame is:

$$\vec{V}(x, r, \theta) = (U, 0, \omega r) \tag{6}$$

To account for the influence of system of vortices introduced into a uniform flow we use Biot-Savart law, according to which the velocity induced by *k*th lifting line can be calculated at any point in the field by:

$$\overrightarrow{v_k}(x, y, z) = \frac{1}{4\pi}\int_{L_k} \frac{\vec{\Gamma} \times \vec{R}}{\left|\vec{R}\right|^3} dl + \frac{1}{4\pi}\int_{S_k} \frac{\vec{\gamma} \times \vec{R}}{\left|\vec{R}\right|^3} dS, \tag{7}$$

where $\vec{R}$ is the position vector that goes from the integration point to the considered field point (x, y, z) with module $\left|\vec{R}\right|$. The integration is performed along the lifting line L_k and the surface of the sheet of trailing vortices shed from this line along the wake, S_k. It is important to remark that when we compute velocities induced only at the lifting lines we can omit first integral – due to the symmetry of the rotor influences of the lifting lines cancel each other out and only the trailing vortices have to be taken into account:

$$\overrightarrow{v_k}(x, y, z) = \frac{1}{4\pi}\int_{Sk} \frac{\vec{\gamma} \times \vec{R}}{\left|\vec{R}\right|^3} dS. \tag{8}$$

The total induced velocity is a sum of contributions of all Z blades, i.e. Z lifting lines and their corresponding vortex sheets:

$$\vec{v}(x, y, z) = \sum_{k=1}^{Z} \overrightarrow{v_k}(x, y, z). \tag{9}$$

Having that established, the total velocity field is a sum of undisturbed flow $\vec{U}_\infty$ (Equation 6) and velocity induced by system of vortices $\vec{V}$, so that in the cylindrical coordinates:

$$\vec{V}(x, r, \theta) = (U - v_a,\ v_r, \omega r + v_t), \tag{10}$$

where v_a, v_r and v_t denote respectively the axial, radial and tangential components of induced velocity and are expressed by:

$$v_a = -v_x, \tag{11a}$$

$$v_r = v_y cos\theta + v_z sin\theta, \tag{11b}$$

$$v_t = -v_y sin\theta + v_z cos\theta, \tag{11c}$$

where θ is the angular coordinate in the $y-z$ plane of coordinate system.

Forces, angles, and coefficients

To discuss forces resulting from interaction between fluid and blades let's recall Kutta-Joukowski theorem (Equation 1):

$$\vec{L} = -\rho\vec{V} \times \vec{\Gamma}. \tag{12}$$

This formula gives lift force per unit span, which, by definition, is perpendicular to the incoming flow. Moreover, as both circulation vector $\vec{\Gamma}$ and radial component of the induced velocity $\vec{v}_r$ are aligned with the lifting line, the cross product $\vec{v}_r \times \vec{\Gamma}$ will be equal to zero. In means that radial components (i.e. parallel to the lifting line) of the induced velocities do not contribute to the lifting force. Following that, the magnitude of the lift force per unit span is expressed by:

$$L = \rho V \Gamma. \tag{13}$$

At each radial position along lifting lines the flow can be assumed as approximately two-dimensional as shown in Fig. 3.

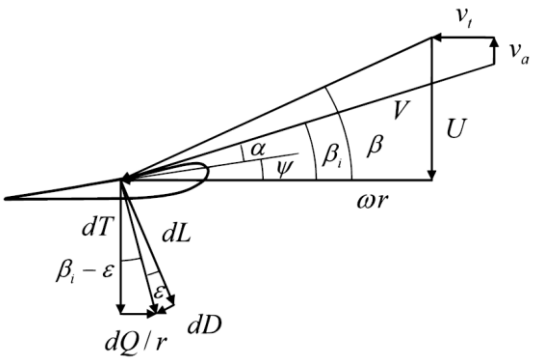

Fig. 3: Velocity and force triangles at a blade section (from [9])

The total velocity experienced by the blade that includes influence of induced velocities is given by:

$$V = \sqrt{(U - v_a)^2 + (\omega r + v_t)^2} \tag{14}$$

Before further analysis of forces, let's identify some angles and forces from Fig. 3. In the velocity triangle:

β – the undisturbed aerodynamic pitch angle:

$$tan\,\beta = \frac{U}{\omega r} = \frac{1}{\lambda r^*}, \tag{15}$$

where $r^* = r/R$ is the dimensionless radius and λ is the tip speed ratio:

$$\lambda = \frac{\omega R}{U}. \tag{16}$$

β_i – the induced aerodynamic pitch angle, which includes the effect of the induced velocities:

$$tan\,\beta_i = \frac{U - v_a}{\omega r + v_t} = \frac{1 - v_a^*}{\lambda r^* + v_t^*}, \tag{17}$$

where $v_{a,t}^* = v_{a,t}/U$ represent dimensionless induced velocities.

α – the angle of attack.

ψ – blade pitch angle, which is the geometrical angle between the blade chord line and the tangential direction, given by:

$$\psi = \beta_i - \alpha. \tag{18}$$

The components of the forces triangle are:

L – lift per unit span,

D – drag per unit span, the consequence of the viscous effects,

T – thrust, axial force aligned with the axis of rotation,

Q/r – circumferential force, which contributes to the torque, acting the tangential direction.

We introduce the dimensionless lift, drag, axial force and power coefficients, expressed respectively by:

$$C_L = \frac{L}{\frac{1}{2}\rho V^2 c} = \frac{2\Gamma}{Vc} = \frac{2\Gamma^*}{V^* c^*}, \tag{19}$$

$$C_D = \frac{D}{\frac{1}{2}\rho V^2 c}, \tag{20}$$

$$C_T = \frac{T}{\frac{1}{2}\rho U^2 \pi R^2}, \tag{21}$$

$$C_P = \frac{P}{\frac{1}{2}\rho U^3 \pi R^2} = \frac{\omega Q}{\frac{1}{2}\rho U^3 \pi R^2}. \tag{22}$$

The star * above the symbol denotes, that the value is dimensionless, thus $\Gamma^* = \Gamma/(UR)$, $c^* = c/R$ and V^* is the dimensionless form of the Equation 14:

$$V^* = V/U = \sqrt{(1 - v_a^*)^2 + (\lambda r^* + v_t^*)^2}. \tag{23}$$

The C_L and C_D are defined in an analogous way and are function of the angle of attack α and the Reynolds number $Re = Vc/\nu$, where ν is the kinematic viscosity of the fluid. Their values are characteristic for a given airfoil and are obtained experimentally or by applying numerical methods. At this point, it is worth to mention an important parameter describing the role of viscous effects, i.e. drag to lift ratio defined by:

$$\varepsilon = D/L = C_D/C_L. \tag{24}$$

Remembering that L is lift force per unit span, for the axial force T we can write equation that relate this force to the circulation Γ, analogous to Equation 13:

$$\frac{dT}{dr} = \rho(\omega r + v_t)\Gamma(r). \tag{25}$$

Now, we have to integrate this formula for axial force per unit span along all Z blades and to account for viscous

effects we introduce ε. In such way we obtain the expression for total axial force:

$$T = \rho Z \int_{r_h}^{R} (\omega r + v_t)\Gamma(r)(1 + \varepsilon \tan\beta_i)\, dr, \tag{26}$$

which substituted to Equation 21 and considered in non-dimensional variables gives:

$$C_T = \frac{2Z}{\pi} \int_{r_h^*}^{1} (\lambda r^* + v_t^*)\Gamma^*(1 + \varepsilon \tan\beta_i)\, dr^*. \tag{27}$$

Following the same steps for the power coefficient we finally get:

$$C_P = \frac{2Z\lambda}{\pi} \int_{r_h^*}^{1} (1 - v_a^*)\Gamma^* \left(1 - \frac{\varepsilon}{\tan\beta_i}\right) r^* dr^*. \tag{28}$$

Modeling of wake expansion

The wind turbine converts kinetic energy of the inflowing fluid into rotational energy of the turbine's rotor. As part of the fluid energy is extracted by the rotor, velocity of the fluid downstream the rotor must decrease compared to the inflow velocity. As the flow is assumed to be incompressible and mass flow must be conserved, slowing down the fluid results in the expansion of the wake.

In order to analyze the effect of the wake expansion we need to point out the following aspects:

- axial position of the end of the expansion zone – the region in which wake is expanding,
- radius of the fully expanded wake,
- function defining the shape of the expanded wake.

Starting with the axial position of the end of the expansion zone x_{ult}, from the theoretical point of view, it should be assigned to the axial station at which the radial component of the induced velocity becomes negligible. However, because of the difficulties related to the practical application of this approach, in the used computational code x_{ult} is not related with any other variable, i.e. it can be arbitrarily imposed as an input parameter. As the variations of the intensity of trailing vortices are more pronounced near the rotor and their influence on the lifting line decrease with the increasing distance it is reasonable to consider lengths of the expansion zone not longer than a few rotor radii e.g. from $x/R = 1$ to $x/R = 5$. Moreover, it seems convenient to couple the end of the expansion zone with the last alignment station, which makes it to coincide with the end of the transition wake and the beginning of the far wake.

To define the radius of the fully expanded wake, we use the actuator disc theory. Fig. 4. shows an actuator disc, which is a theoretical representation of the wind turbine rotor, extracting energy from the uniform inflow with velocity U. Extraction of the kinetic energy slows down the fluid and, together with the mass flow conservation, causes expansion of the stream-tube.

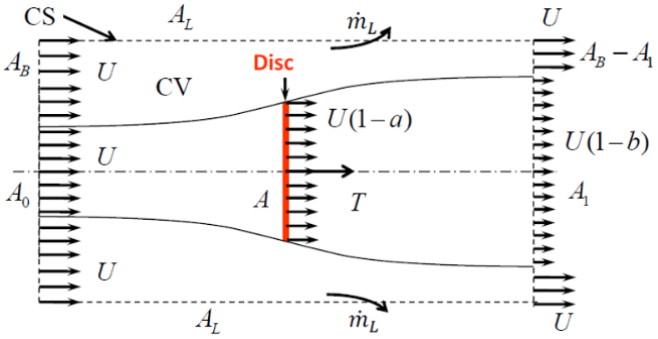

Fig. 4: The actuator disc extracting energy from the fluid and the stream-tube (from [10])

The axial force acting uniformly on a disc is:

$$T = 2\rho A U^2 a(1 - a), \tag{29}$$

where a is the axial flow induction factor. Equation 29 substituted to Equation 21 gives:

$$C_T = 4a(1 - a) \Rightarrow a = \frac{1}{2}\left(1 - \sqrt{1 - C_T}\right). \tag{30}$$

Mass flow rate inside the stream-tube is:

$$\dot{m} = \rho A_{disc} V_{disc} = \rho A_1 V_1 \Rightarrow \frac{A_{disc}}{A_1} = \frac{V_1}{V_{disc}}, \tag{31}$$

where A_{disc}, A_1, V_{disc} and V_1 are surface areas and fluid velocities at the actuator disc and far downstream (i.e. at the boundary of the control volume CV) respectively, given by: $A_{disc} = \pi R^2$, $V_{disc} = U(1 - a)$, $A_1 = \pi R_{max}^2$, $V_1 = U(1 - 2a)$, where R is the radius of the actuator disc (turbine rotor) and R_{max} is the radius of the fully expanded wake. Combining all we obtain the formula for the dimensionless radius of the fully expanded wake:

$$r_{max}{}^* = \frac{R_{max}}{R} = \sqrt{\frac{1}{2}\left(\sqrt{\frac{1}{1 - C_T}} + 1\right)}, \tag{32}$$

which is dependent on the axial force coefficient C_T i.e. on the turbine load.

The non-dimensional radius of the expanded wake will change along the axial coordinate from 1 to $r_{max}{}^*$ according to the expression:

$$r_t{}^*(x) = 1 + (r_{max}{}^* - 1) \cdot f\big(\xi(x)\big), \tag{33}$$

where $f(\xi)$ is a polynomial function. Subscript t indicates that Equation 33 applies to the blade tip.

The expression originally proposed by Hoshino [11] for the contraction of the propeller wakes is adapted for the purpose of the wind turbine wake expansion. The formula, from this point on called occasionally the empirical function, is given by:

$$f(\xi) = \sqrt{\xi} + 1.013\xi - 1.920\xi^2 + 1.228\xi^3 - 0.321\xi^4, \tag{34}$$

with:

$$\xi(x) = \frac{x - x_0}{x_{ult} - x_0}, \tag{35}$$

where x is the axial coordinate at which the expanded radius is computed, and x_0 is the axial station at which the expansion starts. Since expansion starts at the rotor plane $x_0 = 0$ and:

$$\xi(x) = \frac{x}{x_{ult}}. \tag{36}$$

Note, that as x varies from 0 to x_{ult}, value of ξ changes linearly from 0 to 1. Therefore, as an alternative to the empirical function (Equation 34), linear expansion of the wake can be applied simply by replacing Equation 33 with:

$$r_t^*(x) = 1 + (r_{max}^* - 1) \cdot \xi(x). \tag{37}$$

Shapes of the two functions that can be used to expand the wake radius are depicted in Fig. 5.

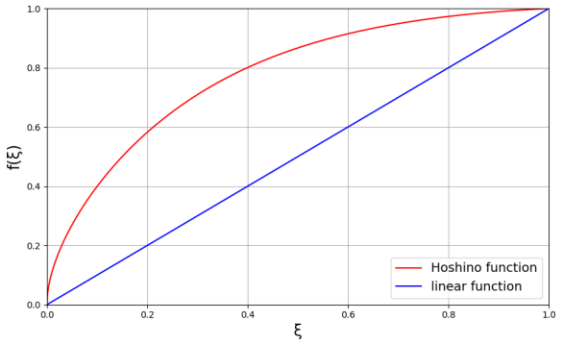

Fig. 5: Functions used to define the shape of the expanded wake

NUMERICAL MODEL

Discretization

From now on all the variables will be non-dimensional, we will cease to use a star superscript *. Lifting line is a bound vortex of varying circulation along its length. As this continuous change cannot be numerically modeled, the lifting line must be discretized into M vortex segments characterized by constant circulation Γ_i. It means, that in the computational procedure the continuous variation of the lifting line intensity is represented in a stepwise manner. Points that bound vortex segments are called *end points* - r_j, and points placed in the center of the segments are called *control points* - $\bar{r}_i$, as shown in Fig. 6.

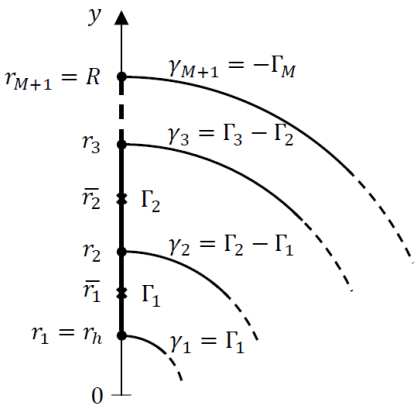

Fig. 6: Discretization of the lifting line (from [5])

Let's remind that in the infinite blade of constant cross-section geometry the circulation is assumed to be constant and the variation of circulation appears in the case of the finite blade, as the circulation at the tip goes to zero. Hence, the gradient of circulation is expected to be larger near the blade tip and it is reasonable to apply a denser discretization in this region. Radial coordinates of the control and end points were computed according to the half-cosine distribution:

$$\bar{r}_i = r_h - (1 - r_h)\cos\left(\frac{\pi/2(i - 1/2)}{M} + \frac{\pi}{2}\right), \quad i = 1, \ldots, M \tag{38}$$

$$r_j = r_h - (1 - r_h)\cos\left(\frac{\pi/2(j - 1)}{M} + \frac{\pi}{2}\right), \quad j = 1, \ldots, M + 1 \tag{39}$$

Wake

In the simpler case without the wake expansion, the wake is assumed to be cylindrical. If we additionally assume constant pitch distribution along the axial direction, we obtain perfectly helicoidal wake vortices and the analytical approach can be applied to compute induced velocities (Morgan and Wrench (1966) computational formulas [12]). The code allows to align the wake at several axial stations, defined among the input parameters. In such case, the wake is characterized by changing its geometry and we need to employ numerical integration in order to compute velocities induced by trailing vortices which are no longer helicoidal. Moreover, the purpose of this work is to examine the influence of the wake expansion which, by definition, assumes a change of the wake geometry and thus excludes considerations of helicoidal wake vortices and the analytical solution. Hence, similarly to the lifting line, the vortex sheet shed downstream to the wake which is theoretically continuous must be discretized into a finite number of concentrated vortices. The lifting line divided into M vortex segments sheds $M + 1$ trailing vortices. Those vortices start at the end points of the lifting line segments, as depicted in Fig. 6, and have intensity equal to the drop of lifting line circulation at the specific points:

$$\begin{gathered} \gamma_1 = \Gamma_1, \\ \gamma_j = \Gamma_j - \Gamma_{j-1}, j = 2, \ldots, M, \\ \gamma_{M+1} = -\Gamma_M. \end{gathered} \tag{40}$$

Each of the $M + 1$ trailing vortices is further discretized into a number of N segments which depends on two input parameters: N_t – the number of streamwise segments equally distributed per one revolution and x_{uw} – the axial coordinate of the ultimate section, where the wake is truncated, defining the axial length of the wake.

To apply numerical integration, the wake geometry must be defined, i.e. cylindrical coordinates of all nodes in the wake mesh must be computed. When computations are done without the wake alignment, the wake geometry is computed only once (*the initial wake*). When the alignment scheme is used, the new wake geometry (*the new wake*) is computed in every iteration and we can distinguish two wake regions:

Transition wake – the zone between the lifting lines ($x = 0$) and the far wake station x_{fw} in which the geometry changes along the axial coordinate and the wake expands. In this region a set of n_s alignment sections is defined ($x_1, \dots, x_{n_s}$) and a far wake station is assigned to the last of them: $x_{fw} = x_{n_s}$. At each alignment section the induced velocities are computed for all $M + 1$ trailing vortices. To compute induced velocities between the alignment sections, linear interpolation along the axial direction is used. Next, the axial and angular coordinates of consecutive vortex segment's end points are computed recursively by:

$$x_{j,n+1} = x_{j,n} + p_{j,n}\left(1 + \frac{v_{t_{j,n}}}{\lambda r_j}\right)\frac{2}{N_t}, \tag{41}$$

$$\theta_{j,n+1} = x_{j,n} + \left(1 + \frac{v_{t_{j,n}}}{\lambda r_j}\right)\frac{2\pi}{N_t}, \tag{42}$$

where p is non-dimensional wake pitch given by $p = \pi r \tan\beta_i$.

Ultimate wake – the zone between the far wake station x_{fw} and the ultimate wake station x_{uw} at which the wake is truncated, as the influence of induced velocities further downstream becomes negligible. In this region v_t and p remain constant and have values computed at x_{fw}. Here the wake is already fully expanded and trailing vortices are helicoidal lines.

Note, that to compute x coordinates, we need p which depends on r. To define *initial wake* for the purpose of the first iteration, while computing x coordinates, we assume the wake to be cylindrical: $r_{j,n+1} = r_{j,n}$. This assumption must be done, as radii computed using the expansion formulas depend on the axial coordinate x. However, at the end of defining *initial wake* new radial coordinates are computed to account for the wake expansion. Similarly, coordinates of the expanded radial coordinates are updated at the end of every iteration when *new wake* is computed.

Expanded radii

Each of n axial wake stations consist of *j* trailing vortices segments' end points. First, we need to compute radii of those points in the fully expanded wake. Next step is to apply the expansion function given by Equation 33, which relate the amount of the expansion with the axial coordinate. Note, that we want to keep the hub radius constant along whole wake i.e. to keep modelling a cylindrical hub. Hence, expansion in radial direction occurs only between the hub and the tip vortex. To prevent hub radius from stretching we use linear transformation and the radial coordinates of fully expanded trailing vortices end points are:

$$r_{max,j} = r_j \cdot C_1 + C_2, \tag{43}$$

where C_1 and C_2 are coefficients given by:

$$C_1 = \frac{r_{max} - r_h}{r - r_h}, C_2 = r_h(1 - C_1), \tag{44}$$

and r_{max} is the fully expanded radius of trailing vortex shed from the blade tip, i.e. maximum radius of the fully expanded wake.

Now, we can discuss how functions used to shape the wake expansion are applied in the computational procedure. As an example, we focus on the expansion with the empirical function 34). The radial coordinate of the n^{th} segment end point of the j^{th} trailing vortex is defined by:

$$r_{j,n} = r_j + \left(r_{max,j} - r_j\right) \cdot f(\xi_n). \tag{45}$$

where $f(\xi)$ is a polynomial function:

$$f(\xi_n) = \sqrt{\xi_n} + 1.013\xi_n - 1.920{\xi_n}^2 + 1.228{\xi_n}^3 - 0.321{\xi_n}^4, \tag{46}$$

and ξ_n coefficient is:

$$\xi_n = \frac{x_n - x_0}{x_{fw} - x_0}, \tag{47}$$

where x_n is the axial coordinate of the n^{th} wake segment, x_{fw} is the far wake station (i.e. the axial coordinate of the end of the expansion zone). We can transform this equation similarly to Equation 35:

$$\xi_n = \frac{x_n}{x_{fw}}. \tag{48}$$

Induced velocities

The induced velocities computational procedure is based on Biot-Savart law (Equation 7) transformed into form:

$$v_{a,t_i} = \sum_{j=1}^{M} C_{a,t_{ij}}\Gamma_j, \tag{49}$$

in which $C_{a,t_{ij}}$ are axial and tangential influence coefficient matrices. Those coefficients are function of the wake geometry. Depending on the needs, two methods can be used to compute the matrices:

Analytical approach – used when alignment scheme is not applied. In such case trailing vortices are perfectly helicoidal and the induced velocities need to be calculated only at the lifting line. Knowing the parameters that define the wake geometry, i.e. number of rotor blades – Z, distribution of control and end points – $\bar{r}_i$ and r_j, and the induced aerodynamic pitch angle – $\tan\beta_i$, we can use Lerbs' analytical expressions (Morgan and Wrench [12], 1966).

Numerical approach – used when wake is aligned and thus its geometry varies along the axial direction. In this case, we apply the numerical integration implemented by Melo [6]. To do so, we discretize Equation 7 to obtain:

$$\vec{v}(x,y,z) = -\sum_{k=1}^{Z}\sum_{i=1}^{M}\frac{1}{4\pi}\left(\int_{r_{j_i}}^{r_{j_{i+1}}}\frac{\vec{e}_r^{\,k}\times\vec{R}}{\left|\vec{R}\right|^3}dr + \int_{L_{j_{i+1}}^k}\frac{\vec{e}_{t_{j_{i+1}}}^{\,k}\times\vec{R}}{\left|\vec{R}\right|^3}ds_{j_{i+1}}^k - \int_{L_{j_i}^k}\frac{\vec{e}_{t_{j_i}}^{\,k}\times\vec{R}}{\left|\vec{R}\right|^3}ds_{j_i}^k\right)\Gamma_i \quad (50)$$

With this formula we can calculate the velocity induced by the system of vortices at any point. The first integral considers the influence of the i^{th} lifting line segment and is solved analytically, while the remaining two account the influence coming from trailing vortices shed from the end points of relevant lifting line segments (from r_{j_i} to $r_{j_{i+1}}$).

The analytical method works well in the simplified cases which do not require wake discretization – it is fast and does not bare high computational costs. The numerical approach allows to introduce the wake alignment and expansion, so it does not constraint the wake geometry. However, it is much more complex which results in a longer and more demanding computation of the solution.

Hub model

We consider finite span blades and thus each of one-dimensional lifting lines (i.e. straight-line bound vortices) representing them must have two boundaries that need to be included in the numerical model. One boundary is the blade tip, where circulation goes to zero. The other one is the rotor hub. In this case we cannot use the same approach as for the tip because the hub constitutes a physical barrier. A convenient solution proposed by Kerwin [13] is to model the hub as a solid cylinder of a radius r_h along the whole wake. To do so, we introduce a system of image vortices which consists of $M + 1$ image vortices, one for each of trailing vortices. Their intensities are symmetrical to the ones of trailing vortices:

$$\gamma_j{}' = -\gamma_j, \quad (51)$$

their radial coordinates are given by:

$$r_j{}' = \frac{{r_h}^2}{r_j}, \quad (52)$$

and their induced aerodynamic pitch angles are:

$$(tan\,\beta_i)_j{}' = (tan\,\beta_i)_j\frac{r_j}{r_j}. \quad (53)$$

The radial component of the velocity induced by such pair of vortices cancels at all points on the surface of the hub modelled as a cylinder of radius r_h [13].

Finally, the hub effect is included in the numerical model by subtraction of image vortex system influence coefficients matrix from the original vortex system matrix:

$$C_{a,t_{ij}}{}^{total} = C_{a,t_{ij}} - C_{a,t}{}'_{ij}. \quad (54)$$

Optimization

The computational code allows to choose between two methods of the optimization.

Classical Optimization:

As explained by Sousa [7], assuming uniform inflow and neglecting viscous forces, the loss of kinetic energy is minimized in the far wake when input to output power ratio is independent of the radial coordinate. If we also assume that $v_a \ll U$ and $v_t \ll \omega r$, which is right in case of light turbine loads, the condition to meet in order to obtain the optimum circulation distribution, called 'Lerbs criterion', is given by:

$$\frac{(tan\,\beta_i)_i}{(tan\,\beta)_i} = constant, i = 1,\dots,M. \quad (55)$$

We denote this constant as l. Remembering Equation 15 we can reformulate this criterion to:

$$\bar{r}_i(tan\,\beta_i)_i = l. \quad (56)$$

Based on those assumptions, following the reasoning of Sousa [7] we arrive at the system of equations used to calculate optimum circulation distribution:

$$\sum_{j=1}^{M}\left(C_{aij} + \frac{\hat{l}}{\bar{r}_i}C_{tij}\right)\Gamma_j + l\lambda = 1, i = 1,\dots,M, \quad (57)$$

$$C_{T_0} = \frac{2Z}{\pi}\sum_{i=1}^{M}\left\{\left(\lambda\bar{r}_i + v_{t_i}\right)(1+\varepsilon_i(tan\,\beta_i)_i)\Delta r_i\Gamma_i\right\}. \quad (58)$$

where Δr_i is the length of the i^{th} lifting line segment.

Lagrange Multiplier Method:

In this method the auxiliary function is defined:

$$H = C_P + l\left(C_T + C_{T_0}\right), \quad (59)$$

and to find maximum power coefficient C_P for a given load C_{T_0} we must impose the conditions:

$$\frac{\partial H}{\partial\Gamma_i} = 0 \wedge \frac{\partial H}{\partial l} = 0, \qquad i = 1,\dots,M, \quad (60)$$

where l is the Lagrange multiplier.

With such assumptions, following the steps described by Sousa [7] we can derive the system of equations that need to be satisfied in this optimization method:

$$\sum_{j=1}^{M}\left\{\begin{bmatrix}-\lambda\left(1-\frac{\varepsilon_i}{(tan\,\beta_i)_i}\right)\left(C_{a_{ij}}\bar{r}_i\Delta r_i + C_{a_{ji}}\bar{r}_j\Delta r_j\right) + \\ +\hat{l}(1+\varepsilon_i(tan\,\beta_i)_i)\left(C_{t_{ij}}\Delta r_i + C_{t_{ji}}\Delta r_j\right)\end{bmatrix}\Gamma_j\right\} + \\ + \{\lambda(1+\varepsilon_i(tan\,\beta_i)_i)\bar{r}_i\Delta r_i\}l = -\lambda\left(1-\frac{\varepsilon_i}{(tan\,\beta_i)_i}\right)\bar{r}_i\Delta r_i, \\ i = 1,\dots,M, \quad (61)$$

$$C_{T_0} = \frac{2Z}{\pi}\sum_{i=1}^{M}\left\{\left(\lambda\bar{r}_i + v_{t_i}\right)(1+\varepsilon_i(tan\,\beta_i)_i)\Delta r_i\Gamma_i\right\}. \quad (62)$$

RESULTS AND DISCUSSION

Convergence

The numerical methods suffer from iterative error, round-off error and discretization error. In this analysis we examine the influence of the latter one on the results. To do so, we check the effect of changing input parameters responsible for the discretization of the wake. As we

focus on the wake alignment and expansion, all tests require the use of the numerical approach. Therefore, the choice of the right values of input parameters is very important for obtaining convergent solutions and minimize the discretization error.

In the convergence analysis we examine the influence of the discretization parameters on the computational model, namely the number of lifting line segments M, the number of streamwise segments per one revolution N_t and the axial end wake station x_{uw}/R. All tests were performed using both expansion methods, and most of them repeated for one and three alignment stations. Some of them were additionally compared with the case without the wake expansion.

General conclusion from this analysis is to keep using the values of the discretization parameters recommended by Sousa, i.e. $M = 30,\ N_t = 100$ and $x_{uw}/R = 25$, as the application of the expansion does not cause the need for the additional adjustments.

Transition wake parameters

The influence of the parameters responsible for the shape of the transition zone on the results was tested. Those are the parameters defining the wake alignment and expansion, i.e. the number and position of the wake alignment stations, length of the expansion zone and the radius of the fully expanded wake.

First, is it important to mention that circulation distribution over the lifting line presented in Fig. 7 shows an expected behavior, which indicates that after the application of the wake expansion the optimization procedure is still successfully performed.

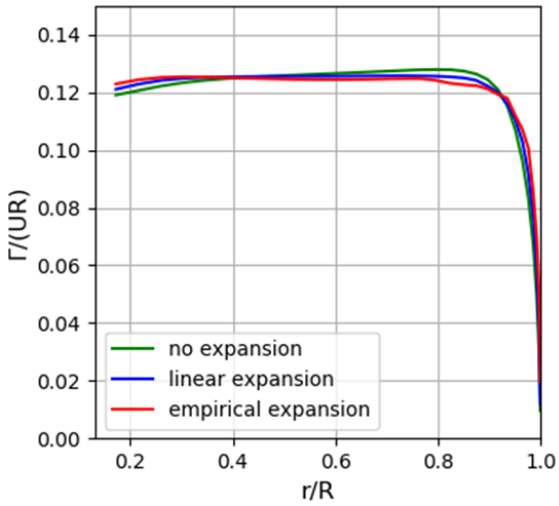

Fig. 7: Circulation distribution obtained with and without the wake expansion

In general, it is recommended to always aim at smooth wake geometries by inspection of the local variables' distributions and the vortex sheet shape. Example of what we understand as good behavior of the wake geometry is presented in Fig. 8.

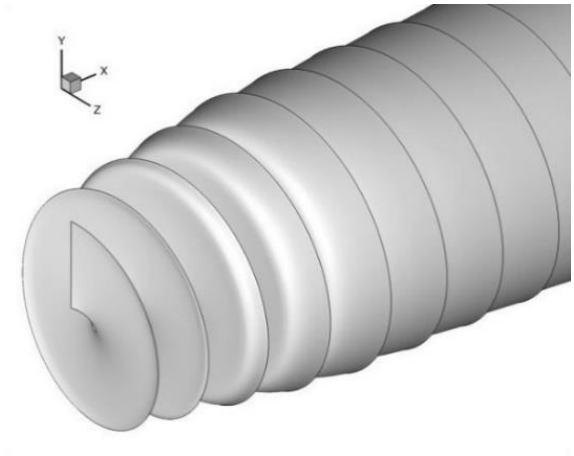

Fig. 8: Geometry of the wake aligned at axial stations $x/R = \{0, 1, 2\}$ expanded with the linear expansion function

Fig. 9 shows how the choice of the wake alignment stations configuration influence the stability of achieved results in terms of the pitch distribution over the lifting line.

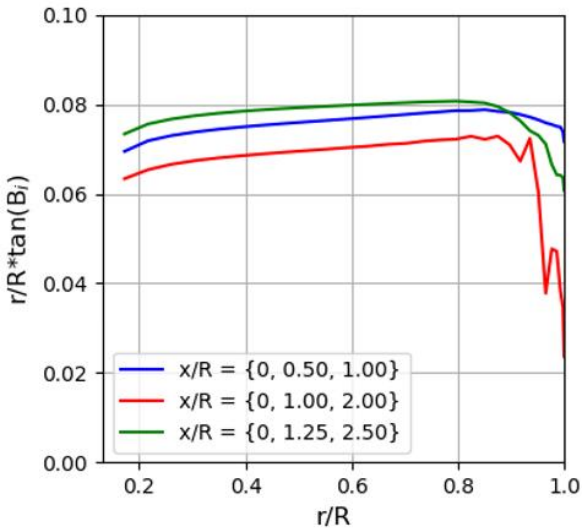

Fig. 9: Induced aerodynamic pitch for different configurations of the alignmens stations for the case without the wake expansion

Tests revealed, that introduction of the wake expansion contributes to the improvement of the results stability in terms of the deigned turbine performance (see Tab. 1) and the optimal configurations of the axial alignment stations are $x\ /\ R = \{0, 1, 2\}$ for the case without, and $x\ /\ R = \{0, 1.25, 2.5\}$ for the case with the wake expansion.

	C_P		
x/R	no expansion	linear expansion	empirical funtion expansion
$\{0, 0.5, 1\}$	0.4292	0.4424	0.4592
$\{0, 0.75, 1.5\}$	0.3795	0.4403	0.4473
$\{0, 1, 2\}$	0.3828	0.4462	0.4463
$\{0, 1.25, 2.5\}$	0.4385	0.4467	0.4474

Tab. 1: Power coefficient for chosen configurations of the wake alignment stations

The other tests showed the dependency of the power coefficient on the maximum radius of the expansion. However, at this stage of the research, there is no reason to use different radius of the expanded wake than the one that can be calculated using Equation 32, so this approach is recommended.

Parametric studies

Up to this point we have been checking the effect of changing the parameters of the computational model itself. Now, we focus on the influence of design parameters such as tip speed ratio λ (see Fig. 10) and drag-to-lift ratio ε (see Fig. 11) on the solution of the model with fixed settings.

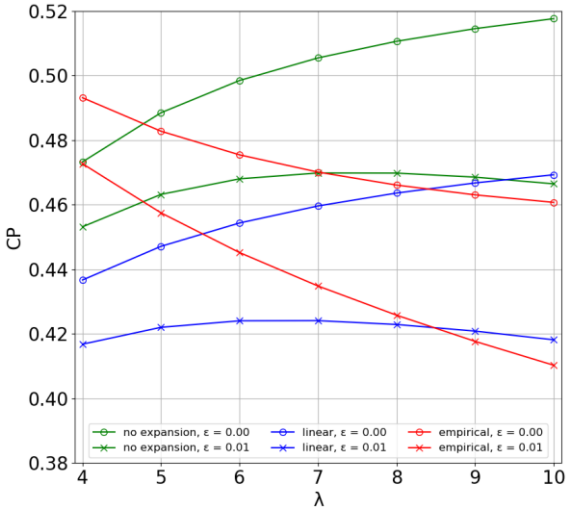

Fig. 10: Effect of the tip speed ratio on the power coefficient – wake aligned at the lifting line only

The curves representing cases without the expansion and with the linear expansion in Fig. 10 show the known result: a monotonic increase of the power coefficient with rising value of the tip speed ratio, described in detail by Sousa [7]. The unexpected results of tests with the use of the empirical function may find explanation in numerical issues caused by a steep slope of the function proposed by Hoshino in the vicinity the lifting line.

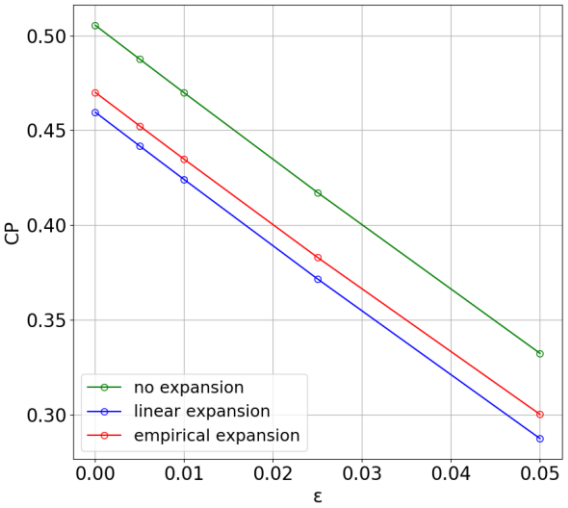

Fig. 11: Effect of the drag-to-lift ratio on the power coefficient – wake aligned at the lifting line only

As for the influence of rising drag-to-lift ratio, it causes almost linear decrease of the power coefficient, depicted in Fig. 11. Such result was also obtained and discussed by Sousa [7]. Similar studies were performed for the cases with three alignment stations. However, most probably due to introduction of additional numerical errors, their readability is strongly reduced.

CONCLUSIONS

The implementation of the wake expansion to the wind turbine design procedure of the lifting line model is presented. The approaches to the wake expansion, together with the relevant theory as well as the details of its practical application are discussed.

The convergence analysis shows that discretization parameters recommended previously by Sousa [7] for the model without the effect of the wake expansion and with the use of an analytical approach are the ones giving sufficient accuracy for a reasonable computational cost.

The parameters of the transition wake are analyzed. The most remarkable conclusion that can be drawn from this study is that input parameters should be chosen carefully for the specific design case. The model is very sensitive to the changes of parameters defining the wake geometry. It is recommended to always control local variables' distributions and the shape of the vortex sheet to obtain smooth wake geometries. Any oscillations caused by the numerical issues are unwelcome and can lead to inaccurate values of the power coefficient.

An interesting remark is that in analyzed cases with two and three alignment stations the introduction of the wake expansion procedure contributes to slightly reduced but more stable and repeatable values of the power coefficient. Moreover, the number of the alignment stations seem to have stronger impact on the expected turbine performance than the position of the last of them (i.e. the length of the transition zone).

Concerning the parametric studies, in the tests with only one alignment station we observe well known dependency of the power coefficient on the value of the design tip speed ratio and drag-to-lift ratio, discussed by Sousa [7]. It is important to notice, that like in the case of the convergence analysis, the introduction of the additional wake alignment stations reduces the readability of the results.

In case of the expansion with the function adapted from Hoshino [11] we face some results which are not coherent with the known research. The function proposed by Hoshino was originally developed to model the contraction of the wake in considerations of the marine propellers. Therefore, the introduction of some adjustments could contribute to the improvement of the results of the procedure in which this function is used for the wake expansion.

There is certainly a lot of room for further improvement of the lifting line code in terms of the wake expansion procedure. First, the additional detailed analysis of the possible expansion functions could lead to finding methods that give more stable and satisfying results. Even more promising approach would be the inclusion of a radial induced velocities in the wake expansion computational procedure, as it would contribute to more realistic geometry of the expanded wakes and open the door for the exploration of the roll-up effect. The other area that could be improved is the numerical procedure itself. Finding more efficient numerical methods could help to achieve higher stability and allow us to decrease the numerical tolerance in order to obtain more accurate results.

ACKNOWLEDGEMENTS

The author would like to thank his superiors – for giving him this opportunity and aiding him with their expert-level knowledge – as well as his family and friends for all their support.

REFERENCES

[1] Theodore von Karman. Aerodynamics: Selected Topics in the Light of Their Historical Development. 2004. ISBN 0486434850.

[2] J. L. Machado. Projecto hidrodinâmico de turbinas de corrente marítima de eixo horizontal com o modelo da linha sustentadora. MSc Thesis in Mechanical Engineering, Instituto Superior Técnico, Universidade de Lisboa, 2010.

[3] J. Baltazar, J. L. Machado, and J. Falcão De Campos. Hydrodynamic Design and Analysis of Horizontal Axis Marine. In ASME 30th International Conference on Ocean, Offshore and Arctic Engineering, Rotterdam, 2011.

[4] J. M. R. Caldeira. Análise de um Modelo de Perda para o Cálculo Aerodinâmico da Turbina Eólica de Eixo Horizontal NREL / NWTC com o Método da Linha Sustentadora. MSc Thesis in Mechanical Engineering, Instituto Superior Técnico, Universidade de Lisboa, 2014.

[5] D. B. Melo. Análise de turbinas de eixo horizontal com o modelo da linha sustentadora. MSc Thesis in Mechanical Engineering, Instituto Superior Técnico, Universidade de Lisboa, 2016.

[6] D. B. Melo, J. Baltazar, and J. A. Falcão de Campos. A numerical wake alignment method for horizontal axis wind turbines with the lifting line theory. Journal of Wind Engineering and Industrial Aerodynamics, 174(January):382–390, 2018. ISSN 01676105. doi: 10.1016/j.jweia.2018.01.028.

[7] Sousa, G. Aerodynamic Optimization of Horizontal Axis Wind Turbines Using the Lifting Line Theory Gonçalo dos Santos Sousa - MSc Thesis in Mechanical Engineering. Instituto Superior Tecnico, 2018.

[8] H. Helmholtz. Über Integrale der hydrodynamischen Gleichungen, welche den Wirbelbewegungen entsprechen. Journal für die reine und angewandte Mathematik, 55:25–55, 1858.

[9] J. L. Machado. Projecto Hidrodinâmico de Turbinas de Corrente Marítima de Eixo Horizontal com o Modelo da Linha Sustentadora. MSc Thesis in Mechanical Engineering, Instituto Superior Técnico, Universidade de Lisboa, 2010.

[10] J. Baltazar, J. A. Falcão de Campos. Offshore Wind Energy Lecture Notes, Instituto Superior Técnico, Universidade de Lisboa, 2019.

[11] T. Hoshino, “Hydrodynamic Analysis of Propellers in Steady Flow using a Surface Panel Method. 2nd Report: Flow Field Around Propeller.,” *Journal of The Society of Naval Architects of Japan*, vol. 166, pp. 79–92, 1989.

[12] W. Morgan and J. Wrench. Some Computational Aspects of Propeller Design. Methods in Computational Physics, 4:301–331, 1965.

[13] J. Kerwin, Lecture Notes on Hydrofoils and Propellers. MIT, Cambridge MA. 2001.